대표7

Qualification Program of Lap Joints for ITER Coils

Yuri Ilyin, Fabrice Simon, Qing Hua, Andrei Baikalov, Chen-Yu Gung, Hyungjun Kim, Bernard Turck, Kazuya Hamada, Sebastien Koczorowski, Nello Dolgetta, Cormany Carl, Enrique Gaxiola, Alexander Vostner, Byung Su Lim, Paul Libeyre, Arnaud Devred, and Neil Mitchell

***Abstract*—The superconducting coils of the ITER magnet system have hundreds of electrical lap joints interconnecting superconducting cables. The joints operate in a magnetic field of up to 4 T, field derivatives of 0.5 T/s, and currents up to 70 kA. The acceptance tests for the toroidal field (TF), poloidal field (PF), and correction coil (CC) coils will be performed at 77 K, before they are assembled in the pit. Hence there will be no possibility to measure the resistance of the joints in the superconducting state before the whole magnet system is enclosed in the Tokamak cryostat. In addition, no reliable nondestructive method has been found to spot the joints with a failure at room temperature. Therefore, the production of the joints relies on the strict adhesion to established robust manufacturing procedures during the qualification phase. As additional quality monitoring, a periodic test of the joint samples manufactured in parallel with a coil fabrication is foreseen to control the reproducibility of the joint electrical performance. In order to qualify the manufacturing procedures, to establish a series production tools and worker teams, a comprehensive qualification program has been set up for manufacturers of the coils in Russia (Poloidal Coil 1, PF1), China (PF6, feeders, CC), Japan (TF), Europe (TF and PF), and USA (Central Solenoid, CS). This program includes a set of mockups manufactured according to the process to be used for the coils and submitted to different tests. They include mechanical testing of materials, electrical tests of full size joint samples, destructive microscopic examination of the joint mockups, and mechanical testing of the full size joint mockups. All tests are carried out in specialized laboratories qualified for this type of work. This paper describes the main items of the qualification program, the tests performed, and the acceptance criteria. The test results are reported and compared to the criteria.**

***Index Terms*—ITER, lap joint, manufacturing procedures, qualification, superconducting coils.**

I. Introduction

THIS paper outlines the qualification activities on the lap joints for the ITER superconducting magnets. In all coils they provide electrical and hydraulic connection between the coil terminals and feeder busbars. In the feeders they interconnect the sections of the busbars. In the TF and PF coils they interconnect the modules called pancakes. In total there are 8 types of conductors on which the lap joints will be fabricated [1].

All lap joints are of the twin-box design, e.g., [2], assembled in either "shaking hands" or "praying hands" configuration.

Manuscript received August 28, 2017; accepted November 15, 2017. Date of publication December 13, 2017; date of current version December 27, 2017. *(Corresponding author: Yuri Ilyin.)*

The authors are with the ITER Organization, St. Paul Lez Durance 13067, France (e-mail: yury.ilin@iter.org).

Color versions of one or more of the figures in this paper are available online at http://ieeexplore.ieee.org.

Digital Object Identifier 10.1109/TASC.2017.2778102

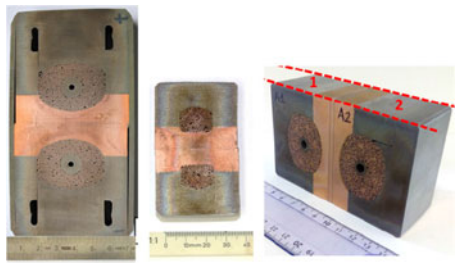

Fig. 1. Family of the twin box joints. Left – PF6 joint by ASIPP (similar design with the MB joint), middle – CC joint by ASIPP, right – TF joint by ASG Superconductors (similar design with the CS joint). The channels in the PF boxes are to allow for full penetration weld of the cover. The copper shim in between the joint boxes is to mitigate assembly tolerances. Courtesy of CERN.

Each half joint represents a leak-tight bi-metallic box with one side made of copper (copper sole). One end of the box is welded to the conductor jacket. Inside the box, the strands on the cable periphery are free of Ni/Cr coating and either silver plated, tinned or with the bare copper surface. The strands in contact with the copper sole are either soldered to or pressed into the sole. The cable is compacted with a box cover to a $\sim 20\%$ void fraction in the strands region to ensure low and steady electrical resistance of the joints. The cover is then sealed with welds and two copper sides of the boxes are soldered or compressed together with the indium wires in between to form the joint. Examples of the joints' cross-sections are shown in Fig. 1. The differences in the joint design among the coils are summarized in Table I. They arise from the functional requirements of the joints, manufacturing route for the coils and experience of the manufacturers. For example, the joints for the TF conductors and CS leads will be heat treated at $\sim 650\,^{\circ}\mathrm{C}$ to form Nb_3Sn in the strands. In those joints the low resistive interface between the strands and the copper sole is formed by diffusion bonding. No solder or strand/copper coating is allowed. As another example, for the most mechanically loaded PF and feeder joints with NbTi strands it was decided to provide additional mechanical strength to the strands-copper and box-box interfaces by soldering them together. In the feeder joints it has been changed to indium bonded interfaces for the sake of manufacturing simplicity [2], but the same could not be applied to the PF coil joints because of the elevated temperatures for the epoxy resin curing.

Currently all the coil and feeder manufacturers led by the five ITER Domestic Agencies entered into the production phase meaning they successfully had passed the qualification phase for the critical components, the joints being one of them. The objective of the qualification phase aims at demonstrating that the

TABLE I
DESIGN PARAMETERS OF ITER LAP JOINTS

	PF	Feeder MB/CB	CC	TF	CS
Void fraction, %	19 ± 1	21 ± 1	22 ± 1	21 ± 1	22 ± 1
Ni/Cr removal method	brush/PF6 reverse plating	Reverse plating	brush	brush	brush
Box annealing prior to use	no	no	no	4 h at 400 C	no
SS wraps btw petals	preserved	n/a	n/a	removed	preserved
Outermost strands plating	pure tin	Silver	Silver	no	no
Cu sole inner side plating	pure tin	silver + In tinned	Silver	no	no
Cable-sole interface	soldered Sn96Ag4	pressed	Pressed	pressed, sintered	pressed, sintered
Box-box interface	soldered Pb60Sn40 (In wires to feeder)	pressed, In wires	pressed, In wires	soldered Pb60Sn40 (In wires to feeder)	pressed, In wires
Central pipe id/od, mm	3/12	MB: n/a CB: 3/6	n/a	6/10	3.5/9
Sole RRR at 0 T, after bonding and HT (CS/TF)	5 ÷ 6 Copper C12200	70 ÷ 100 Copper C10200/ C12200	70 ÷ 100 Copper C10200	450 ÷ 500 Copper C10100/ C10200	170 ÷ 230 Copper C10200
Jacket-box/ cover-box welds	FP/FP	MB: FPB, CB: FT/FPB	FPB/PP	FT/PP	FT/ PP
Joint clamps, connected by	side plates, weld	brackets, weld	brackets, weld	brackets, weld	brackets, weld

The flat side of the copper sole is either electroplated (PF) or hot tinned (TF) with Pb60Sn40 prior to soldering. All terminal boxes are silver plated on the flat side. The feeder boxes for the TF and CS terminals will be with copper C12200. The TF EU coil boxes will be with copper C10200. PP is partial penetration weld, FPB – full penetration butt weld, FT – fillet weld.

TABLE II
MANUFACTURERS OF MATERIALS FOR JOINT BOXES

Coil	Copper	316L/LN Stainless steel	Cladding
PF1	MKM, GmbH, Germany	Forgiatura Morandini Srl, Italy	"Energometall", Russia
PF2–5	KME Germany AG & Co KG	Fomas Group, Italy	High Energy Metals, USA
MB/CC/PF6	Aurubis, Finland	Guizhou Aerospace Xinli Forging & Casting, China	Nanjing LeiHui New Material China
TF EU	Aurubis, Finland	316L, Outokumpu Stainless AB, Sweden	High Energy Metals, USA
TF JA	Mitsubushi Shindoh, Japan	316LN, Daido Steel Co. Ltd., Japan	Asahi Kasei Corp., Japan
CS	CSN Carl Schreiber, Germany	VDM Metals GmbH, Germany	Nobelclad, France

manufacturing procedures, operators, tools and quality system are mature to minimize the production risks and guarantee successful performance of the component. To qualify the manufacturing procedures for the complicated lap joints, whose electrical, mechanical and vacuum performances are interlinked, a comprehensive programme relying on the manufacture and tests of several mock-ups was set up for all manufacturers.

II. QUALIFICATION ITEMS, CRITERIA, AND RESULTS

A. Materials

Table II summarizes the joint material suppliers for each coil. The bimetallic boxes are made from explosively bonded modified 316L or 316LN (CS, TF) stainless steel and copper hot rolled or forged plates. The stainless steel is the same grade as used in the conductor jackets [1]. The copper unified numbering system (UNS) for different joints is given in Table I and is procured under ASTM B152. The 100% volumetric inspection of the copper-steel interface of each bi-metallic plate is conducted by ultrasonic technique (UT) with calibration to 1.6 mm diameter flat bottom hole (FBH). The area with single indications (peaks in the data) exceeding 1.6 mm in its longest dimension or rounded indications separated by less than 1.6 mm is scrapped. The strength of the bonded interface is checked in the tensile and shear tests of samples extracted from each plate, and should exceed the strength of the copper. In addition, each bar stock interface is checked by dye penetrant: the linear indications and isolated non-linear indications with a diameter above 1 mm are not acceptable.

Any chemicals used in joint manufacturing are requested to be halogen free ($<$50 ppm) to eliminate the risk of corrosion.

B. Strands-Copper and Box-Box Interfaces

These interfaces are critical, as they contribute the most to the joint resistance [3]. Two techniques are used to remove the Ni or Cr coatings from the outer strands: by a rotating stainless steel brush or by reverse electroplating method. When the brush is used, the quality of the removal is controlled visually by comparing the strands' colour with a reference sample. If a manufacturer selects the reverse plating method (either with a sponge or in a bath), the experimentally determined value of the integral of (time $\times$ current) is the acceptance criterion.

In the feeder, CC or PF joints the adhesion of the Ag or Sn plating to the cable and copper sole is measured by the tape test according to ASTM D3359. The adhesion is accepted if no plated material is peeled off by the tape. As an additional control, a plated strand is extracted from the cable, coiled around a 3 mm core, cooled down to 77 K, and then its surface morphology is examined microscopically. Flaking is not acceptable.

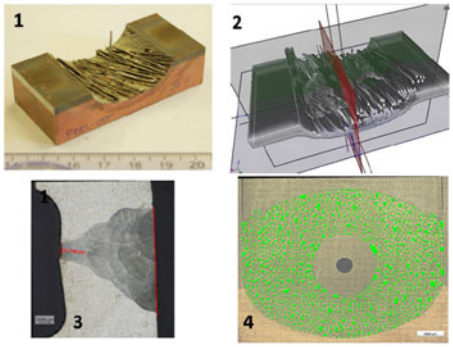

Fig. 2. Tests of the joint samples performed at CERN: 1 – peel-off test on a strand of the PF5 sample manufactured by ASG Superconductors, 2 – re-constructed image by computed tomography to check the number of soldered strands, 3 – macro image of the cover weld slice, 4 - void fraction measurements on the PF6 sample manufactured by ASIPP. The bright colour areas correspond to voids. Courtesy of CERN.

The soldered and indium bonded interfaces between the cable and the copper sole were qualified in the peel off test of single strands, Fig. 2. The bonding is considered satisfactory if the failure mode is predominantly cohesive fracture. In few PF and main busbar (MB) prototype joints analysed destructively by CERN [4] it was found that with the traction angle of 90° and 30 mm long sample the peel off force on a single strand is in average 4–8 N for both soldered and indium interfaces. The computed tomography performed by CERN on the PF5 and PF6 joint samples revealed that at least 90% of the strands at the interface layer are soldered to the sole.

To qualify the soldering procedure of two boxes with a shim in between, the manufacturers had to solder two- and three-plate copper samples of the same size as the copper sole ($10 \times 64 \times 450$ mm) using the same soldering station as for the joint. The two-plate samples were radiographically tested to measure the void area in the solder layer which is accepted if below 20% [3], whilst the second sample was cut in sections of 25 mm width for the shear test. The shear strength of the bonding in the samples is accepted if it is above 5 MPa (the criterion is derived from the statistics on samples with less than 20% voids).

Insufficient sensitivity of the NDT methods [5]–[7] developed for the quality control of the discussed interfaces forced the manufacturers of the PF and TF coils to reconsider their production quality control strategy. It was decided to manufacture and electrically test two full size joint samples per coil and solder a production proof sample followed by destructive examination prior to soldering the joint boxes on the coil.

C. Welds

There are two types of closure welds in all joints – the weld between the conductor jacket and the joint box and between the box and its cover, both manual TIG. The weld to the jacket is the most fatigue loaded one in the PF and MB joints. In the PF coils it transfers the load originated from the coil deformation [8]. In all coil terminals it transfers the load from the feeder buses. The weld process qualification is done to ISO15614-1. The highest quality level B defined in ISO5817 is required for all welds. Each weld is visually inspected, He-leak tested in a

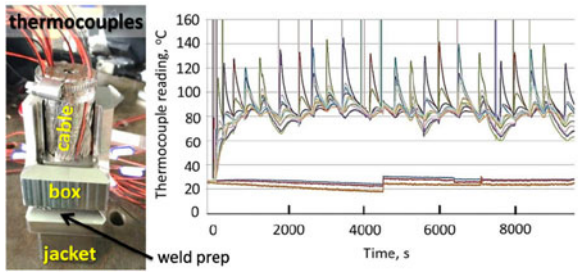

Fig. 3. Left: mock-up of the PF6 joint instrumented with the thermocouples type *K* to monitor the temperature of the strands right under the weld prep during welding. Right: temperature chart recorded during the welding. The peaks of the temperature are below 150 °C. Courtesy of ASIPP and F4E.

local vacuum chamber at 3 MPa pressure inside the box, and dye penetrant tested. The ultrasonic testing (UT) is applied on the full penetration welds of the PF joints and of the cover welds on the MB and correction busbar (CB) joints. Digitally focused arrays (DFA) are used in combination with the compressive wave and shear wave techniques per ISO17640 and ISO22825 allowing detection of the minimum defect of 1 mm. On the TF jacket-box fillet welds the UT is used to check the weld penetration depth.

The requirement for the strands temperature to remain below 250 °C during welding adds up complexity to the welder. Dedicated samples (Fig. 3, [9]) instrumented with the thermocouples to measure the strands' temperature have been manufactured to tune the welding parameters and idle time between the runs for cooling down the welds.

In case of the 2 mm thin wall conductor jackets of MB, TF, CC and CB and with the presence of the cable next to weld seam, the UT is not practical. To validate the quality of the weld manufacturing process in MB and CB, a fatigue tensile test at the operating load was performed on 4 full-size specimens of the weld to 223,000 cycles [2]. Similar tests on the TF and CC fillet welds are ongoing. The quality of the welds during series production is assured by welding of a production proof sample followed by destructive examination before the welder is allowed to work on the coil.

D. Fatigue Test of Full Size Joint Samples

The PF and feeder joints are most demanding in terms of mechanical strength. The manufacturers of those joints built a full size joint sample and tested it under tensile fatigue load. The MB full size joint sample was first cooled down to measure the resistance, then fatigue loaded at room temperature, and finally the electrical test was repeated and revealed no change in the joint resistance [2]. The PF joints were cycled from 7×10^{-5} to 7×10^{-4} linear strain on the conductor jacket ($F_{peak} = 250$ kN, 145 MPa) for 600,000 cycles (20x design life time) or from 7×10^{-5} to 14×10^{-4} during 30,000 cycles whichever suited the manufacture's schedule and cost. A typical sample of the PF5 joint manufactured for mechanical tests is shown in Fig. 4. Before the fatigue test, the samples are cooled down 5 times to 77 K and checked for He leak tightness. After the fatigue test at 77 K, the samples are leak tested again and cut into sections,

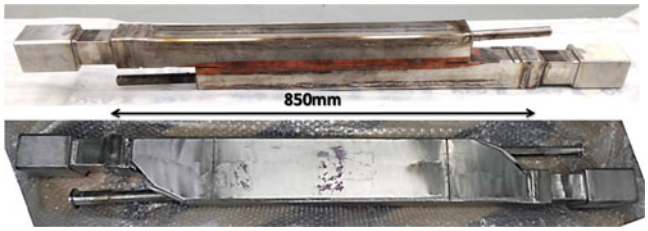

Fig. 4. PF5 dummy joint by ASG Superconductors for mechanical testing. Top: soldered boxes. Bottom: the same boxes with welded end wedges and side plates. Courtesy of ASG Superconductors and F4E.

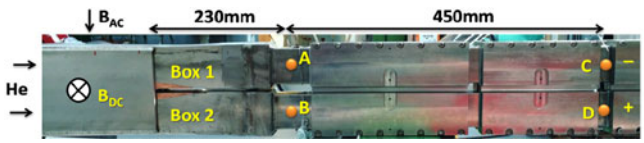

Fig. 5. A part of the Sultan sample of the PF5 type conductor. In the test dwell the sample is oriented vertically with the joint at the bottom. The helium is supplied to the joint pipes, with independently adjustable flow rate in the legs. The voltage is measured between taps on two legs: A and B ("short V-taps") and C-D ("long V-taps)." A-B is at 230 mm from the region where the current transfer begins. The thermometers measuring the conductor jacket temperature are at the locations C and D (downstream). With the Sultan field B_{DC} direction and current polarity as indicated, the load on the boxes is repulsive with the maximum at A-B and decreasing to zero at the end of the joint where the axial component of the current vanishes. Courtesy of ASG Superconductors and F4E.

the soldered layer between the boxes and void fraction in the strands region. The considerable part of the activities on the destructive examination was performed at CERN, e.g., [10], Fig. 2. The results of the void fraction measurements are collected in Table I. The suppliers of the PF5 and PF6 coils successfully tested their joints in KIT (Germany) and SWIP (China) correspondingly. The PF1 coil supplier tested the prototype joint sample in TSNIITMASH (Russia) successfully and is building the qualification sample.

E. Electrical Performance

Each coil supplier manufactured at least one qualification full size joint tested in the SULTAN test facility, Switzerland ([3], [10]–[16], Fig. 5 or in NIFS test facility, Japan ([17], [18]). The feeder like MBJIO1 sample was built in the ITER workshop MIFI in collaboration with ASIPP, China [11], [12]. The qualification samples of the MB, CB, CC and HTS current leads joints built and tested by ASIPP are described in [2], [19], [20]. The acceptance criteria for DC resistance are 5 nΩ at 55 kA and 3 T for PF, 3 nΩ at 68 kA and 2 T for TF, 4 nΩ at 45 kA and 4 T for CS, 2 nΩ at 70 kA and 0 T for MB, 5 nΩ at 10 kA and 2.5 T for CC/CB.

The data presented in Figs. 6 and 7 show that all tested samples satisfy the acceptance criteria with the record low resistance of the MB joint. The PF joints are intentionally ([21], [22]) the most resistive ones with the (calculated) copper contribution to resistance of 70–80%. Then the contribution of the strand-copper interface ranges from 0.5 to 2.5 nΩ for all joints. The bigger resistance in the CC joint [15] compared to MB one with the same copper RRR and strand type is linked to the size of the cable-copper contact area. Variation of the resistance with the

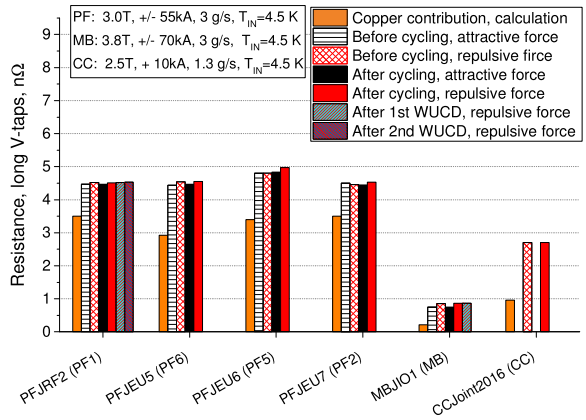

Fig. 6. Resistance of the NbTi joints. The name of the sample is followed up by the conductor type in parenthesis. Electromagnetic (EM) cyclic load for PF joints: 1000 cycles, 5 T, 0/+33 kA, for MB: 1000 cycles, 7 T, −38/+38 kA, and for CC: 2.5 T, 0/+12 kA. PFJ2RF2 sample is manufactured by SNSZ/Efremov, Russia, PFJEU5 – by ASIPP, China, PFJEU6 and PFJEU7 – by CNIM, France, MBJIO1 – by IO/CEA, CCJoint2016 – by ASIPP.

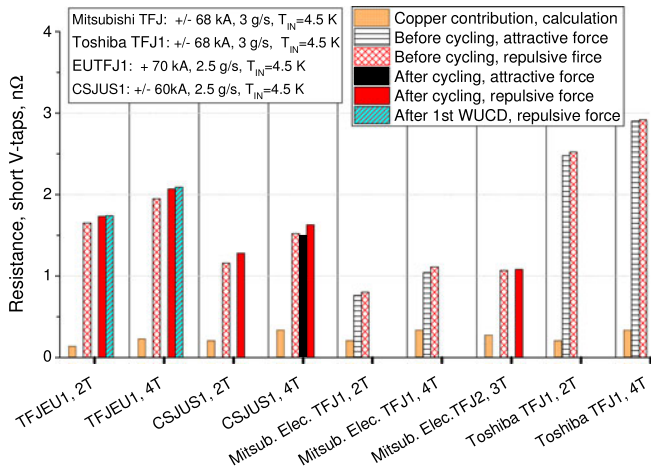

Fig. 7. Resistance of the Nb_3Sn joints (TF and CS conductors). The name of the sample is followed up by the conductor type in parenthesis. Cyclic load for EUTF: 1000 cycles, 8 T and 0/+26.25 kA; for Mits. Elec.: 500 cycles at 35 kA, 7.5 T. TFJEU1 sample was manufactured by ASG Superconductors (Italy), CSJUS1 – by General Atomics (USA).

current is negligible for all joints. Sensitivity of the resistance with the magnetic field is minimal in the PF joints due to low copper RRR. Any visible change with the magnetic field is attributed to the magneto-resistivity of the strands' copper. The Nb_3Sn joint resistance increases by 20–25% between 2–4 T. All joints demonstrate slight increase of the resistance with the cyclic load. In the PF and MB joints we observed saturation of the resistance after already 100 cycles, see Fig. 8 (the difference in *V-short* and *V-long* is discussed in [23]). The resistance of the joints is insensitive to the direction of the force on the boxes, either attractive or repulsive, for practical purpose.

There are no acceptance criteria for the level of the AC losses however they were routinely measured in SULTAN (CC - in the University of Twente [24]) with the AC field transverse to the box-box interface plane on all samples to build a database for the simulations of heat loads in magnet operation, Fig. 9. The characteristic coupling currents time constant $n\tau$ at the origin,

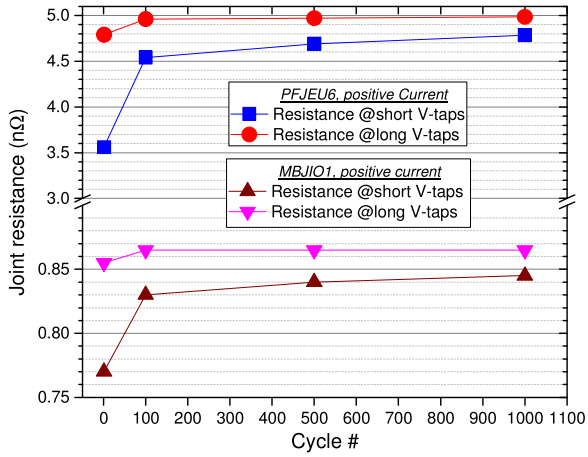

Fig. 8. Typical evolution of joint resistance vs. number of EM cycles for NbTi joints. Higher resistance and earlier saturation is observed on the *long V-taps* which are taken as reference for the joint resistance.

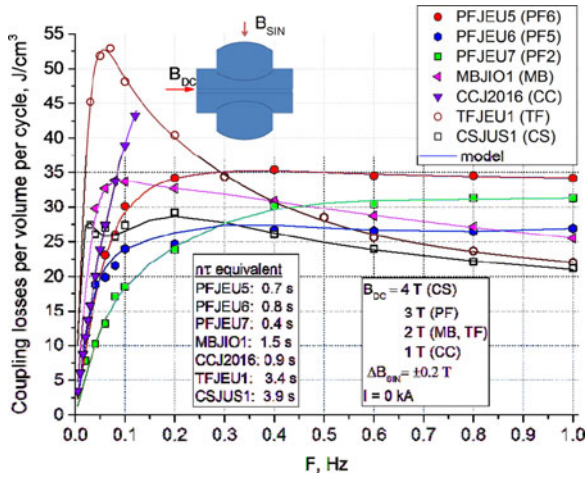

Fig. 9. Coupling losses per unit volume per cycle under sinusoidal field with the amplitude 0.2 T. The normalizing volume is calculated as the total envelop area of the two cables and the copper sole times 390 mm length of the field produced by pulsed coils. The characteristic $n\tau$ is related to this volume.

derived from the fit of the loss curves with [25], decreases with the increase of RRR. However the contribution of the well compacted cable to the losses is not negligible and leads to bigger $n\tau$ and earlier saturation of the loss curve in the PF joints compared to predicted 0.15 s [21]. Despite the higher than expected losses, all PF joints do not quench at the plasma initiation conditions of 0.4 T/s field ramp in 1 s (field transverse to the interface plane) followed by a plateau at 6 K, 3 T background field and 55 kA (see Fig. 10). This corresponds to 55 W peak power and total 70 J energy release in the joint.

When the temperature increased slowly in the NbTi joints at fixed current and field, the quench occurred at the conductor next to the joint nearly at the current sharing temperature predicted for a single strand with the scaling from [27]. This is a strong evidence of the good stability and current sharing of the joints despite that only 50–60% of all strands have a contact with the copper sole. Table III summarizes the parameters at quench of different samples.

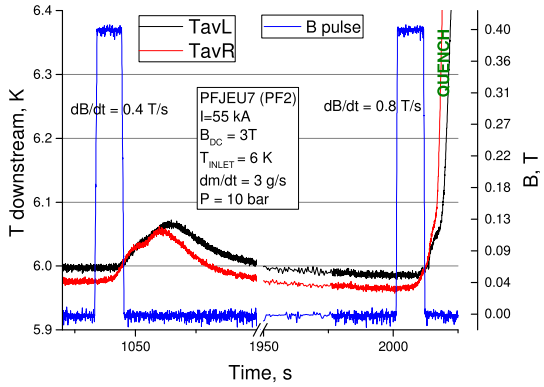

Fig. 10. Stability run on PFJEU7 (PF2) joint. Trapezoidal field pulses with the field direction transverse to the box interface plane with 0.4 T/s and 0.8 T/s are applied at 6 K inlet temperature, 55 kA, 3 g/s mass flow rate and 3 T background field. The conductor near the joint is stable at the joint operating conditions of 0.4 T/s.

TABLE III
TEST PARAMETERS OF NBTI JOINTS AT QUENCH

	PFJEU5	PFJRF2	PFJEU6	PFJEU7	MBJIO1	CCJ2016
Current I_J, kA	55	55	55	55	70	10
# SC strands	1440	1440	1152	720	900	300
dm/dt, g/s	3	3	3	3	3	1.3
B_{DC}, T	3	3	3	3	3.8	2.5
B_{PEAK}, T	3.59	3.59	3.59	3.59	4.55	2.75
T_{IN}, K	6.5	6.65	6.71	6.42	6.5	7.6
T_{OUT}, K	7.08	7.02	7.03	6.85	6.5	7.6
T_{CS} strand, K	7.22	7.22	7.10	6.95	6.45	7.55

T_{IN} and T_{OUT} are measured. B_{PEAK} (the sum of the SULTAN field and sample's self field) is transverse to strands and is calculated at the outermost layer of strands. The current polarity in the experiment is such that the forces on the boxes are attractive and the self-field direction in the midplane between the conductors is opposite to the Sultan field. The current sharing temperature, T_{CS}, is calculated with B_{PEAK} and $I_{STR} = I_J/N\_strands$ and using scaling formulas with the parameters from strand manufacturers.

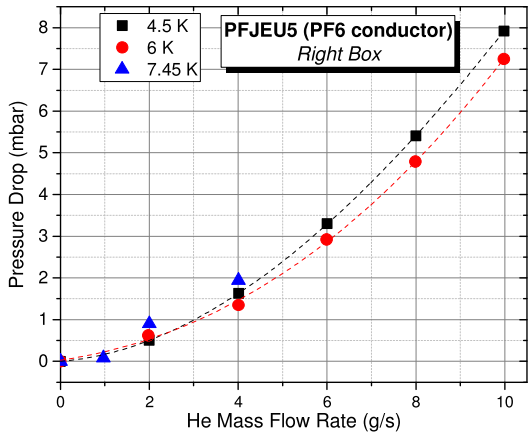

Fig. 11. Pressure drop vs helium mass flow rate and inlet temperature measured by capillaries over one box of the PF6 conductor joint manufactured by ASIPP. The inlet pressure is 10 bar.

F. Pressure Drop

The pressure drop was measured on the most flow resistive PF and MB boxes with the capillaries on both sides of the joint box. The results for the PF6 box are shown in Fig. 11 and for the MB box are reported in [2], [11]. The measured 8 mbar is equal to the pressure drop over 6 m of the PF6 conductor in operating

conditions. This is 3% of the total pressure drop on the smallest PF1 coil, which is conveniently acceptable. The flow test on the PFJEU5 in CEA [28] demonstrated that no less than 70% of the total flow cools the strands region.

III. Conclusion

Prior to start the fabrication of the joints on the conductors, a broad program of qualification of the materials and manufacturing steps was set up for the coil suppliers. Each qualification is achieved through manufacture and tests of prototypes. The electrical performance is qualified by testing the full size joints in nominal operating conditions and above. The mechanical robustness is qualified by testing the full size joints or the samples of the critical welds in fatigue at 77 K. The core qualification program has been successfully completed by all coil suppliers with few remaining items to be finalized in 2017.

Acknowledgment

The work presented in this paper is the joint effort of ITER Organization, ITER Domestic Agencies and many companies and research centres. The authors are indebted to P. Bruzzone, B. Stepanov, K. Sedlak (SPC), A. Bonito-Oliva, K. Smith, P. Valente, C. Sborchia, G. Romano (F4E), R. Penco, P. Pesenti, G. Vercelli, F. Ortona (ASG Superconductors), N. Bugada, F. Chastel, (CNIM), S. Sgobba, S. Langeslag, I. A. Santillana, P. Fernandez (CERN), K. P. Weiss (KIT), A. Nijhuis, J. Huang, T. Bagni (University of Twente), A. Ustinov (RFDA), I. Rodin, E. Marushin, A. Mednikov (D.V. Efremov Institute), E. Niu (CNDA), G. Shen, B. Hu, J. Wei, L. Wang, K. Lu, C. Liu, X. Wen (ASIPP), W. Reiersen, N. Martovetsky (USIPO), J. Smith (JA), P. Decool, and B. Peluso (CEA).

Disclaimer: The views and opinions expressed herein do not necessarily reflect those of the ITER Organization.

References

[1] A. Devred *et al.*, "Status of ITER conductor development and production," *IEEE Trans. Appl. Supercond.*, vol. 22, no. 3, Jun. 2012, Art. no. 4804909.

[2] Y. Ilyin *et al.*, "Design and qualification of joints for ITER magnet Busbar system," *IEEE Trans. Appl. Supercond.*, vol. 26, no. 4, Jun. 2016, Art. no. 4800905.

[3] B. Stepanov, P. Bruzzone, S. March, and K. Sedlak, "Twin-box ITER joints under electromagnetic transient loads," *Fusion Eng. Des.*, vol. 98–99, pp. 1158–1162, Oct. 2015.

[4] S. A. E. Langeslag, CERN, Genève, Switzerland, private communication, 2017.

[5] S. March, P. Bruzzone, K. Hamada, A. Foussat, A. Bonito-Oliva, and M. Cornelis, "Applicability of non-destructive examination to ITER TF joints," *IEEE Trans. Appl. Supercond.*, vol. 25, no. 3, Jun. 2015, Art. no. 4200505.

[6] X. Sarasola, P. Bruzzone, and K. Hamada, "Non-destructive examination method for the ITER Toroidal field conductor terminations," *IEEE Trans. Appl. Supercond.*, vol. 27, no. 4, Jun. 2017, Art. no. 0600305.

[7] T. Hemmi *et al.*, "New inspection method of joint resistance at room temperature for ITER TF coil," *IEEE Trans. Appl. Supercond.*, submitted for publication.

[8] F. Simon, C. Boyer, Y. Ilyin, C. Beemsterboer, and B. S. Lim, "Design of the ITER PF coil joints," *IEEE Trans. Appl. Supercond.*, vol. 22, no. 3, Jun. 2012, Art. no. 4804104.

[9] X. Wen *et al.*, "Research of butt welding of thin-wall jacket for superconducting cable and joint," *Fusion Eng. Des.*, vol. 100, pp. 269–273, Nov. 2015.

[10] L. Wang *et al.*, "Qualification of ITER correction coil superconductor joint," *IEEE Trans. Plasma Sci.*, submitted for publication.

[11] H. Kim *et al.*, "Status and qualification test of feeder main Busbar joint for ITER magnet system," *IEEE Trans. Appl. Supercond.*, submitted for publication.

[12] B. Peluso and R. Piccin, "MIFI (Magnet infrastructure facilities for ITER): activities overview," *IEEE Trans. Appl. Supercond.*, submitted for publication.

[13] E. Marushin *et al.*, "The PF1 coil electrical joint test results," *IEEE Trans. Appl. Supercond.*, submitted for publication.

[14] V. I. Bondarenko *et al.*, "Technology and tooling to manufacture low-ohm (<2 nΩ) electrical joints of the ITER PF1 coil," *IEEE Trans. Appl. Supercond.*, vol. 23, no. 3, Jun. 2013, Art. no. 4201605.

[15] P. Libeyre *et al.*, "Qualification of the manufacturing procedures of the ITER correction coils," *IEEE Trans. Appl. Supercond.*, vol. 27, no. 4, Jun. 2017, Art. no. 4201405.

[16] N. Martovetsky *et al.*, "Performance of the ITER CS joints," *IEEE Trans. Appl. Supercond.*, submitted for publication.

[17] S. Imagawa *et al.*, "Test of ITER-TF joint samples with NIFS test facilities," *IEEE Trans. Appl. Supercond.*, submitted for publication.

[18] H. Kajitani *et al.*, "Evaluation of ITER TF coil joint performance," *IEEE Trans. Appl. Supercond.*, vol. 25, no. 3, Jun. 2015, Art. no. 4202204.

[19] L. Huajun, W. Yu, W. Weiyue, L. Bo, S. Yi, and G. Shuailess, "Experiment of low resistance joints for the ITER correction coil," *Rev. Sci. Instrum.*, vol. 84, no. 1, Jun. 2013, Art. no. 015106.

[20] X. Huang *et al.*, "Design and test results of joints for ITER TF feeder current leads and superconducting Busbars," *IEEE Trans. Appl. Supercond.*, vol. 20, no. 3, pp. 1722–1724, Jun. 2010.

[21] Y. Ilyin *et al.*, "Simulations of twin-box joints for ITER PF coils," *IEEE Trans. Appl. Supercond.*, vol. 24, no. 3, Jun. 2014, Art. no. 9001905.

[22] Y. Ilyin *et al.*, "Analysis of ITER PF coil joint design under reference operating scenario," *IEEE Trans. Appl. Supercond.*, vol. 26, no. 4, Jun. 2016, Art. no. 4201305.

[23] A. Baikalov, Q. Hua, Y. Ilyin, B. S. Lim, and F. Simon, "Analyses of the ITER Poloidal coil joints cold test results," oral presentation at MT-25.

[24] A. Nijhuis, University of Twente, Enschede, The Netherlands, 2017.

[25] B. Turck and L. Zani, "A macroscopic model for coupling current losses in cables made of multistages of superconducting strands and its experimental validation," *Cryogenics*, vol. 50, pp. 443–449, 2010.

[26] J. Huang, T. Bagni, Y. Ilyin, and A. Nijhuis, "Pulsed field stability and AC loss of ITER NbTi PF joints by detailed quantitative modeling," *IEEE Trans. Appl. Supercond.*, submitted for publication.

[27] L. Muzzi *et al.*, "Test results of a NbTi wire for the ITER poloidal field magnets: A validation of the 2-pinning components model," *IEEE Trans. Appl. Supercond.* vol. 21, no. 3, Jun. 2011, pp. 3132–3137.

[28] P. Decool, CEA Cadarache, St. Paul Lez Durance, France, private communication, 2017.